chemosensors

MDPI

Article

Dissolved Gas Analysis in Transformer Oil Using Ni Catalyst Decorated $PtSe_2$ Monolayer: A DFT Study

Zengting Wang [1], Guozhi Zhang [1,2,*], Li Liu [1], Yunjian Wu [1], Jincong Wang [1] and Song Xiao [3]

[1] School of Electrical and Electronic Engineering, Hubei University of Technology, Wuhan 430068, China; 102110366@hbut.edu.cn (Z.W.); li.liu@hbut.edu.cn (L.L.); wuyunjian@hbut.edu.cn (Y.W.); wangjc@hbut.edu.cn (J.W.)
[2] Hubei Engineering Research Center for Safety Monitoring of New Energy and Power Grid Equipment, Wuhan 430068, China
[3] School of Electrical Engineering and Automation, Wuhan University, Wuhan 430072, China; xiaosong@whu.edu.cn
* Correspondence: zhangguozhi@hbut.edu.cn

Abstract: In this paper, the first-principles theory is used to explore the adsorption behavior of Ni catalyst decorated $PtSe_2$ (Ni-$PtSe_2$) monolayer toward the dissolved gas in transformer oil, namely CO and C_2H_2. Some Ni atoms from the catalyst are trapped in the Se vacancy on the pure $PtSe_2$ surface. The geometry configurations of Ni-$PtSe_2$ monolayer before and after gas adsorption, the electronic property of Ni-$PtSe_2$ monolayer upon gas adsorption, and the sensibility and recovery property of Ni-$PtSe_2$ monolayer are explored in this theoretical work. Through the simulation, the E_{ad} of CO and C_2H_2 gas adsorption systems are calculated as −1.583 eV and −1.319 eV, respectively, both identified as chemisorption and implying the stronger performance of the Ni-$PtSe_2$ monolayer on CO molecule, which is further supported by the DOS and BS analysis. According to the formula, the sensitivity of Ni-$PtSe_2$ monolayer towards CO and C_2H_2 detection can reach up to 96.74% and 99.91% at room temperature (298 K), respectively, which manifests the favorable sensing property of these gases as a chemical resistance-type sensor. Recovery behavior indicates that the Ni-$PtSe_2$ monolayer is a satisfied gas scavenger upon the noxious gas dissolved in transformer oil, but its recovery time at room temperature is not satisfactory. To sum up, we monitor the status of the transformer to guarantee the stable operation of the power system through the Ni-$PtSe_2$ monolayer upon the detection of CO and C_2H_2, which may realize related applications, and provide the basis and reference to cutting-edge research in the field of electricity in the future.

Keywords: Ni-$PtSe_2$ monolayer; first-principles theory; dissolved gas in transformer oil; gas scavenger

Citation: Wang, Z.; Zhang, G.; Liu, L.; Wu, Y.; Wang, J.; Xiao, S. Dissolved Gas Analysis in Transformer Oil Using Ni Catalyst Decorated $PtSe_2$ Monolayer: A DFT Study. *Chemosensors* **2022**, *10*, 292. https://doi.org/10.3390/chemosensors10080292

Academic Editor: Eleonora Alfinito

Received: 12 June 2022
Accepted: 16 July 2022
Published: 25 July 2022

1. Introduction

Transformers, which are static induction appliances using the principle of electromagnetic induction to change alternating current voltage and transmit alternating current power, are widely applied in modern industrial enterprises. Transformers can be classified as dry-type transformers, oil-immersed transformers, and gas-filled transformers. The oil-immersed transformer, an indispensable piece of electrical equipment in the modern era, accounts for more than 90% of all types of transformers and is of great significance in practical applications [1–3]. Although transformer oil is a petroleum-based liquid that has the possibility of burning and has disadvantages in environmental protection, most power transformers still use it as insulation and a cooling medium, for it possesses the characteristics of excellent insulation performance, low viscosity, admirable heat transfer performance, reduces the aging of insulation materials, and is of low price [4–6].

However, after long-term running, several transformer faults, such as the overheating of insulation oil, partial discharge, arc discharge, spark discharge, water ingress and dampness, natural aging, and so on, will give rise to great influence on the power system and

may cause immeasurable economic losses [7–9]. These phenomena will bring on the breakage of certain C-C and C-H bonds in the transformer oil in the environment of electricity and heat, with a small number of active hydrogen atoms and unstable hydrocarbon free radicals emerging, which are further reorganized into hydrogen (H_2) and low molecular hydrocarbons, such as methane (CH_4), ethane (C_2H_6), ethylene (C_2H_4), acetylene (C_2H_2), and CO, CO_2, and other gases [10–12]. Among these by-products, the content of CO and C_2H_2 accounts for most of all the gases [13]. Therefore, it is quite essential to monitor online whether the transformer is operated normally by means of detecting the main components of decomposition gases of transformer oil, namely CO and C_2H_2.

Over recent years, two-dimensional (2D) layered materials such as graphene and transition metal dichalcogenides (TMDs), have attracted the attention of researchers around the world on account of their strong chemical reactivity to various gas species. With the discovery of graphene, a growing amount of related research has appeared in the fields of digital information, field-effect devices, biomedicine, and sensing materials for its high thermal conductivity, admirable charge mobility, and large specific surface area [9,14,15]. Likewise, TMDs such as MoS_2 which is widely studied, are also favorable 2D materials and possess outstanding performance in gas sensing [3,16–21]. Among all those TMDs, platinum diselenide ($PtSe_2$) monolayer, as another member of 2D-layered materials, exhibits eminent semiconductor property since the band gap of its monolayer is about 1.2 eV [22,23]. Besides, several research reports indicate that the $PtSe_2$ monolayer possesses excellent performance in detecting gas molecules on the basis of the first-principles theory [22,24]. Even so, we need to make use of transition metal (TM) doping to improve the electron redistribution of the whole system and further enhance the sensitivity and responsiveness in gas interaction, since the binding force between the gas molecule and the $PtSe_2$ monolayer is not enough to bring on electron transfer between the two [22]. Moreover, it is propitious for the filling of the doped atoms that the lattice constant and the bond length between atoms in $PtSe_2$ monolayer are larger than that in MoS_2 monolayer [25–28]. It is reported that the Ni atom, as a dopant, possesses favorable catalytic property and electron mobility in gas interactions, imposing a significant promotion for gas detection. Therefore, it is reasonable for us to assume a Ni-doped $PtSe_2$ (Ni-$PtSe_2$) monolayer as a promising novel sensing material to explore its sensing potential toward the main parts of dissolved gas in transformer oil based on first-principles theory. This theoretical work will be quite significant for the stable operation of the power system and provide a critical reference to future scientific studies.

2. Computational Details

In this work, the total geometric and electronic calculations on the basis of first-principles theory were carried out in the DMol^3 package [29]. The Perdew-Burke-Ernzerhof (PBE) function within the generalized gradient approximation (GGA) was taken to conduct the exchange correlation interaction [30]. DFT-D2 method proposed by Grimme was chosen to correct dispersion to consider the Van der Waals force and long-range interactions [31]. The Monkhorst-Pack *k*-point mesh of $10 \times 10 \times 1$ was adopted for the Brillouin zone integration [32]. We selected the energy tolerance accuracy, maximum force, and displacement to be 10^{-5} Ha, 2×10^{-3} Ha/Å, and 5×10^{-3} Å [33], respectively. Self-consistent loop energy of 10^{-6} Ha, global orbital cut-off radius of 5.0 Å, and smearing of 0.005 Ha were applied to ensure the accuracy of the total energy [34].

We establish a $4 \times 4 \times 1$ $PtSe_2$ monolayer supercell to perform the whole first-principles calculations, which include 16 Pt atoms and 32 Se atoms with a vacuum region of 15 Å to prevent the possible interactions between the adjacent units [35] since previous studies have shown that a $4 \times 4 \times 1$ supercell would be large enough to conduct the gas adsorption process [10]. The lattice constant of the optimized pristine $PtSe_2$ monolayer

was obtained as 3.71 Å, in accordance with data from previous research reports [36]. The adsorption energy (E_{ad}) was calculated by

$$E_{ad} = E_{Ni-PtSe_2/gas} - E_{Ni-PtSe_2} - E_{gas} \quad (1)$$

where in $E_{Ni-PtSe_2/gas}$, $E_{Ni-PtSe_2}$ and E_{gas} were the energies of the gas adsorbed system, isolated Ni-$PtSe_2$ monolayer and gas molecule, respectively. The Hirshfeld method was adopted to consider the charge-transfer (Q_T) between the target molecule and the adsorbent surface, which is proposed to describe carried electron value by gas molecule after adsorption. Only the most stable configurations (MSC) for gas adsorption would be plotted and discussed below.

3. Results and Discussion

3.1. Analysis of Ni-$PtSe_2$ Monolayer and Gas Species

As shown in Figure 1, we optimize CO and C_2H_2 molecules to their most stable geometry structure, where we mark the bond length for the sake of better comparing the changes before and after gas absorption. One can see from Figure 1a,b, that with sp orbital hybridization in CO and C_2H_2, the C-O bond in CO (1.142 Å) is longer than the C-H bonds in C_2H_2 (1.071 Å) for the reason of the smaller radius of H atom than O atom. Likewise, since the larger radius of the C atom than the O atom, the C-C bond in C_2H_2 (1.211 Å) is longer than the C-O bond in CO.

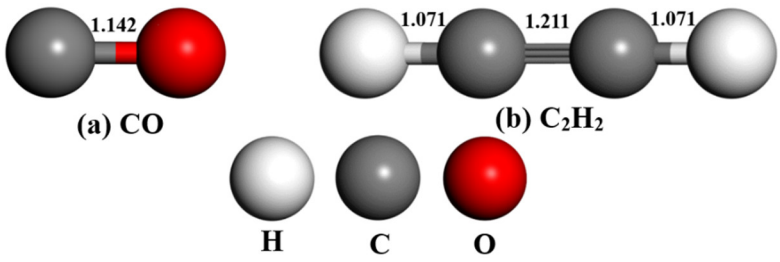

Figure 1. Geometric structures of gas molecules. (**a**) CO, (**b**) C_2H_2.

After theoretical calculations, we found that the E_{ad} of pristine $PtSe_2$ monolayer adsorbing CO and C_2H_2 are 0.26 and 0.21 eV, respectively. The magnitude of the interaction between the pristine $PtSe_2$ monolayer and the gas molecules during the adsorption process is quite weak. Therefore, the pristine $PtSe_2$ monolayer is not suitable as a sensing material for detecting CO and C_2H_2.

It is a known fact that mono-sulfur vacancy is the most occurred point defect structure in the TMDs [18,37]. Recently, it is proven that the Se vacancy in $PtSe_2$ monolayer is usually easier to be formed than the Pt vacancy [38,39]. The lattice constant and interatomic bond length of the $PtSe_2$ monolayer is relatively large, which is conducive to replacing the filling of atoms. Therefore, it is reasonable to speculate that the enhanced response of the $PtSe_2$ monolayer to the gas molecules can be achieved by atomic doping. Figure 2a exhibits the structurally optimized Se-vacancy from $PtSe_2$ monolayer. It can be seen that the geometry around the Se vacancy is slightly deformed compared with the intrinsic structure that the Se-Pt bond length around the Se vacancy is shortened by 2%, due to the Se vacancy in the $PtSe_2$ monolayer. Besides, as shown in Figure 2b, the MSC is formed by Ni atom doping in the Se vacancy after structural optimization. The Se-Pt bond length is restored to a large extent in the Ni-$PtSe_2$ system. This finding shows that the geometry of the $PtSe_2$ monolayer, which can be restored by filling the vacancy with other atoms is deformed by the presence of Se vacancy. This finding is consistent with that demonstrated in the MoS_2 system [17]. In order to determine the chemical stability of the Ni-$PtSe_2$ monolayer, the value of E_{ad} between Ni atom and S vacancy $PtSe_2$ monolayer was calculated. The result shows that the binding strength of the Ni-$PtSe_2$ monolayer (−4.50 eV) is much higher than that of

the intrinsic $PtSe_2$ monolayer, indicating that its chemical stability is greatly improved compared to that of the intrinsic $PtSe_2$ monolayer [22]. It can be seen from the front view and top view in Figure 2b, that the Ni dopant forms three new chemical bonds with three neighboring Pt atoms, namely Ni-Pt bonds, which are all shorter than the pristine Se-Pt bond length. The position of the Ni atom is also slightly lower than the Se atomic plane from the top view on account of the smaller radius of the Se atom than the Ni atom. This also indicates the deformation of the geometric structure upon the $PtSe_2$ monolayer caused by the Ni dopant.

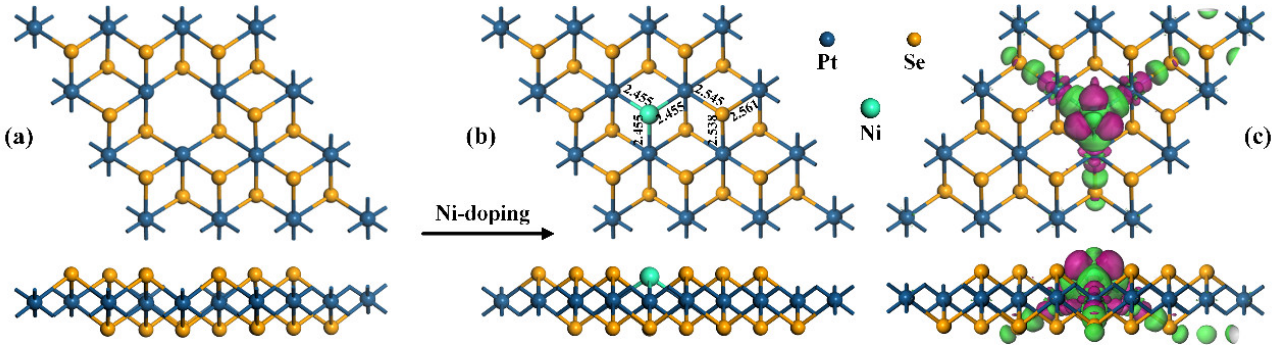

Figure 2. Ni doping process on the $PtSe_2$ monolayer with Se-vacancy. The MSC of (**a**) the $PtSe_2$ monolayer with Se-vacancy: (**b**) Ni-$PtSe_2$ monolayer; and (**c**) related EDD of Ni-$PtSe_2$ monolayer. In EDD, the green (rosy) areas indicate electron accumulation (depletion).

Based on the Hirshfeld analysis, it can be found that the carried charge of the Ni dopant is −0.0823 e, which manifests that the Ni atom behaves as an electron recipient, charging 0.0823 e from the $PtSe_2$ monolayer with Se-vacancy. Se atoms serve as electron acceptors while Pt atoms as electron contributors in the doping process. As we can see from Figure 2b, where electron density difference (EDD) of $PtSe_2$ monolayer is exhibited, the green electron accumulation is mainly concentrated around the Ni dopant and the Se atoms, while the rosy electron depletion around the Pt atoms. These phenomena exhibit the electron hybridization between the Ni dopant and the adjacent atoms during the doping process, and meanwhile also are in accordance with the electron transfer property in the Hirshfeld analysis.

In order to explore the effect on the electron behavior of the Ni atom doping on the $PtSe_2$ monolayer, Figure 3 exhibits the band structure (BS) and density of state (DOS) of the Ni-$PtSe_2$ system by means of simulation. As we all know, we can judge the electrical conductivity of certain materials by the band gap. The widening of the band gap corresponds to a decrease in conductivity, otherwise, the opposite is true [40–42]. According to the research, the bandgap of the pristine $PtSe_2$ monolayer which is an indirect semiconductor is about 1.2 eV [23]. While the calculated bandgap for the Ni-$PtSe_2$ system shrinks down to 0.849 eV compared to the intrinsic $PtSe_2$ monolayer, this indicates that doping of the Ni atom can improve the electrical conductivity of the pristine $PtSe_2$ monolayer and Ni-$PtSe_2$ monolayer takes on the metallic properties. One can see from Figure 3b where the DOS of the $PtSe_2$ monolayer with Se-vacancy and Ni-$PtSe_2$ systems are both exhibited, several novel peaks emerge from the DOS curve of the $PtSe_2$ monolayer with Se-vacancy attributed to the doping of Ni dopant, bringing on the remarkably increased states of Ni-$PtSe_2$ monolayer at the Fermi level, from which the conclusion can be drawn that the conductivity of Ni-$PtSe_2$ has been enhanced. Besides, the DOS curve of the Ni-$PtSe_2$ monolayer is shifted to the right and a lower region compared with the $PtSe_2$ monolayer with Se-vacancy, since the electron-contributing behavior of the $PtSe_2$ monolayer. From the partial DOS of Figure 3c, the Ni 3d orbital overlap constantly with the Se 3p orbital from—6.5 to 2 eV, demonstrating the strong electron hybridization between the Ni and Se atoms on account of the electron transfer, which further verifies the formation of new chemical bonds, namely Ni-Pt bonds.

Above all, the Ni dopant has generated a significant impact on the geometric structure of the pristine $PtSe_2$ monolayer, which will lead to a higher conductivity.

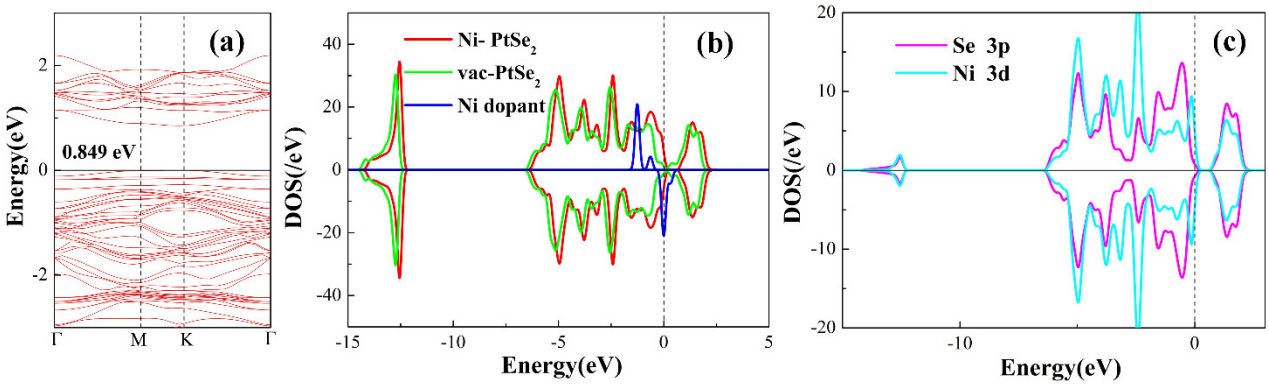

Figure 3. (**a**) BS of the Ni-$PtSe_2$ system, (**b**) DOS comparison, and (**c**) partial DOS. The value in the BS is the bandgap, and the dashed line in DOS is the Fermi level.

3.2. Gas Adsorption Configurations on Ni-Ptse$_2$ Monolayer

Various gas adsorption configurations were established for the sake of exploring whether the Ni-$PtSe_2$ monolayer possesses eminent sensing and adsorbing performance toward the dissolved gas in transformer oil. From Figure 4a, where the most stable geometric structure for CO adsorption onto the Ni-$PtSe_2$ surface is depicted, the CO molecule lies diagonally above the Ni atom, with the plane of Ni-$PtSe_2$ monolayer into a slope. The C atom of CO is captured by the Ni dopant, generating the new chemical bond, namely the C-Ni bond, with a bond length of 1.769 Å. The average Ni-Pt bond length is obtained as 2.560 Å, longer than that in the isolated Ni-$PtSe_2$ system. The C-O bond length elongates from 1.142 Å to 1.158 Å. These phenomena manifest interaction between the Ni-$PtSe_2$ monolayer and CO molecule, giving rise to apparent deformation toward the geometric structure of the Ni-$PtSe_2$ monolayer in the process of gas absorption. It is pointed out that the C-Ni bond length (1.769 Å) is shorter than the covalent radii (1.92 Å) between the C atom and Ni atom, which is consistent with the conclusion that the CO adsorption system is classified as chemisorption, since E_{ad} is calculated as −1.583 eV, larger than the reference value. According to the research [43], the interaction mechanism can be determined as physical adsorption when the E_{ad} is between 0.1 and 0.6 eV, and chemical adsorption when the E_{ad} is greater than 0.8 eV. The E_{ad} is an important parameter to measure the strength of the adsorption effect during adsorption reaction based on the first-principles theory, which can directly indicate the magnitude of the interaction between the adsorbent and the adsorbed substrate during the adsorption process.

Furthermore, based on charge partitioning by the Hirshfeld method, the CO molecule performs as an electron acceptor, withdrawing 0.0079 e from the Ni-$PtSe_2$ monolayer. The Ni dopant as an electron embracer, carries 0.133 e from the Ni-$PtSe_2$ monolayer during gas absorption, accounting for its strong electron receptivity. As depicted in Figure 4b, the CO molecule and Ni atom are mainly surrounded by the green electron accumulation, manifesting their electron-accepting behavior, whereas, the rosy depletion around the Pt atom demonstrates its electron-loss property in the CO adsorption system. Massive green electron accumulation on the C-Ni bond verifies the electron hybridization between the C atom and Ni atom. These phenomena are in accordance with the above Hirshfeld analysis.

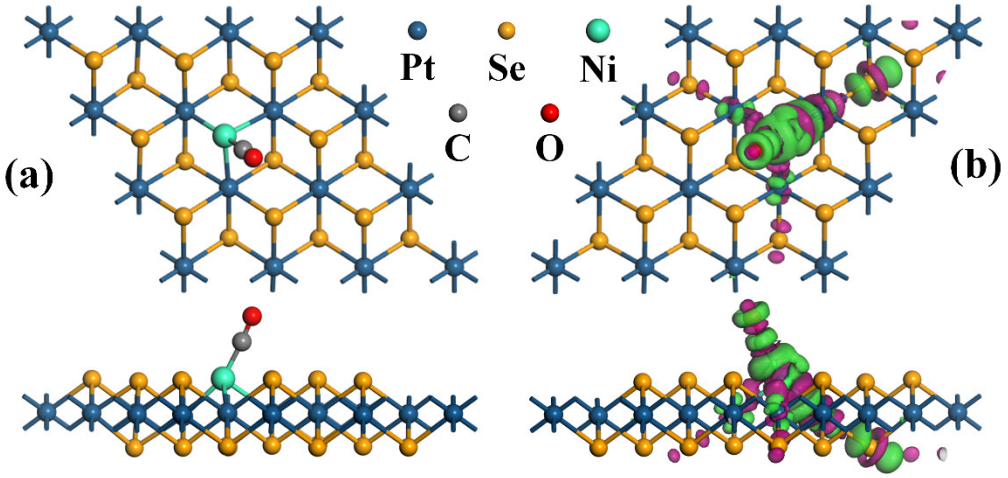

Figure 4. (**a**) The MSC, (**b**) EDD of Ni- $PtSe_2$/CO system. In EDD, the green (rosy) areas indicate electron accumulation (depletion).

For the C_2H_2 adsorption system, the different views of MSC, as well as EDD, are exhibited in Figure 5. It can be found that the C_2H_2 molecule traps in the Ni-$PtSe_2$ surface, with the parallel position and a small slope to the Ni-$PtSe_2$ plane, forming two new Ni−C covalent bonds whose bond length are 1.948 Å and 1.915 Å, respectively, much larger than the length of covalent radii of Ni and C atoms (1.92 Å). Severe deformation occurs after the C_2H_2 molecule is absorbed into the Ni dopant, the linear structure of the C_2H_2 molecule, namely the C≡C bond, gets stretched, and elongated from 1.211 Å to 1.262 Å, which shows that the C_2H_2 molecule is highly activated during gas adsorption. Moreover, chemisorption can be confirmed in the C_2H_2 adsorption system, on account of the simulation result that the calculated E_{ad} is −1.319 eV, larger than the critical value of 0.8 eV. Based on the Hirshfeld analysis, the C_2H_2 molecule transfers 0.0281 e to the Ni-PtSe2 surface, while the Ni dopant as a catalyst withdraws 0.1183 e as well as the Se atom receiving electrons during gas adsorption, which implies the electron-donating property of C_2H_2 molecules. In the EDD, it is obvious that the strong green electron accumulations are mainly situated at the newly formed Ni−C bonds and the Ni dopant, which demonstrates not only the formation of Ni−C bonds but also the electron-accepting behavior of the Ni dopant in C_2H_2 adsorption. The rosy electron depletions are mainly located on the Ni−Pt and C≡C bonds, which implies the weakness of the Ni−Pt and C≡C bonds, in line with the elongation of C≡C bonds and Ni−Pt bonds after the C_2H_2 is absorbed.

On all accounts, the Ni dopant plays a significant impact on electron redistribution toward the above two various gas absorption systems. We can infer that the Ni-$PtSe_2$ monolayer conducts strong chemisorption on CO and C_2H_2, with its adsorption strength upon two gases in the order CO > C_2H_2, judging by the value of E_{ad}.

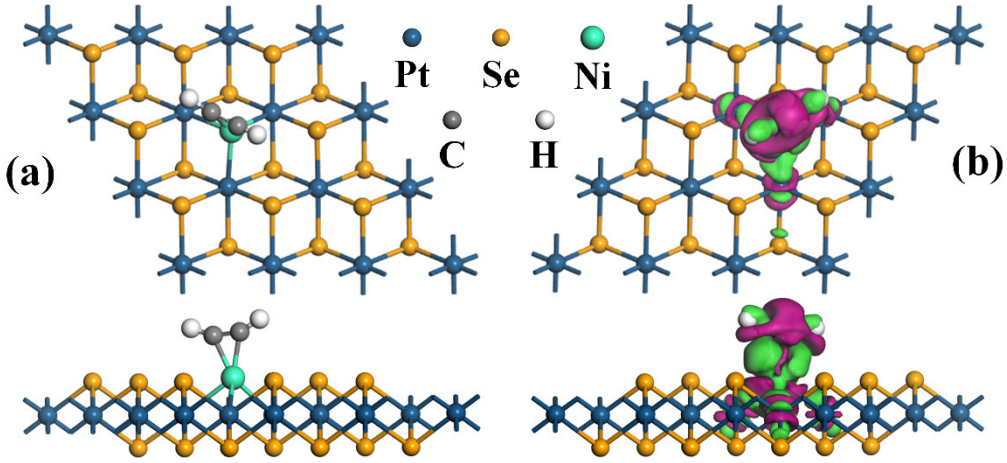

Figure 5. (**a**) The MSC, (**b**) EDD of Ni-$PtSe_2$/C_2H_2 system. In EDD, the green (rosy) areas indicate electron accumulation (depletion).

3.3. Electronic Property of Ni-Ptse$_2$ Monolayer upon Gas Adsorption

The BS and DOS of CO and C_2H_2 systems are exhibited in Figure 6 to further analyze the electronic behavior of the Ni-$PtSe_2$ monolayer upon gas adsorption. We can clearly find that the bandgap of the Ni-$PtSe_2$ monolayer is calculated as 0.673 eV and 0.489 eV, respectively, after adsorption of CO and C_2H_2 molecules, less than that of 0.849 eV in the pristine Ni-$PtSe_2$ system, which implies that the electrical conductivity of the Ni-$PtSe_2$ monolayer has been enhanced with different amplitude in various adsorption systems. It is worth pointing out that the descending order of the bandgap in these systems is C_2H_2 > CO, contrary to the order of E_{ad}: CO > C_2H_2. Since the smaller molecule, which is more likely to be trapped in the Ni dopant, leads to the stronger binding force of the Ni−C bond, corresponding to the larger E_{ad}. Therefore, a conclusion can be drawn that the CO adsorption system matched with a larger bandgap possesses superior sensing response properties than the C_2H_2 system.

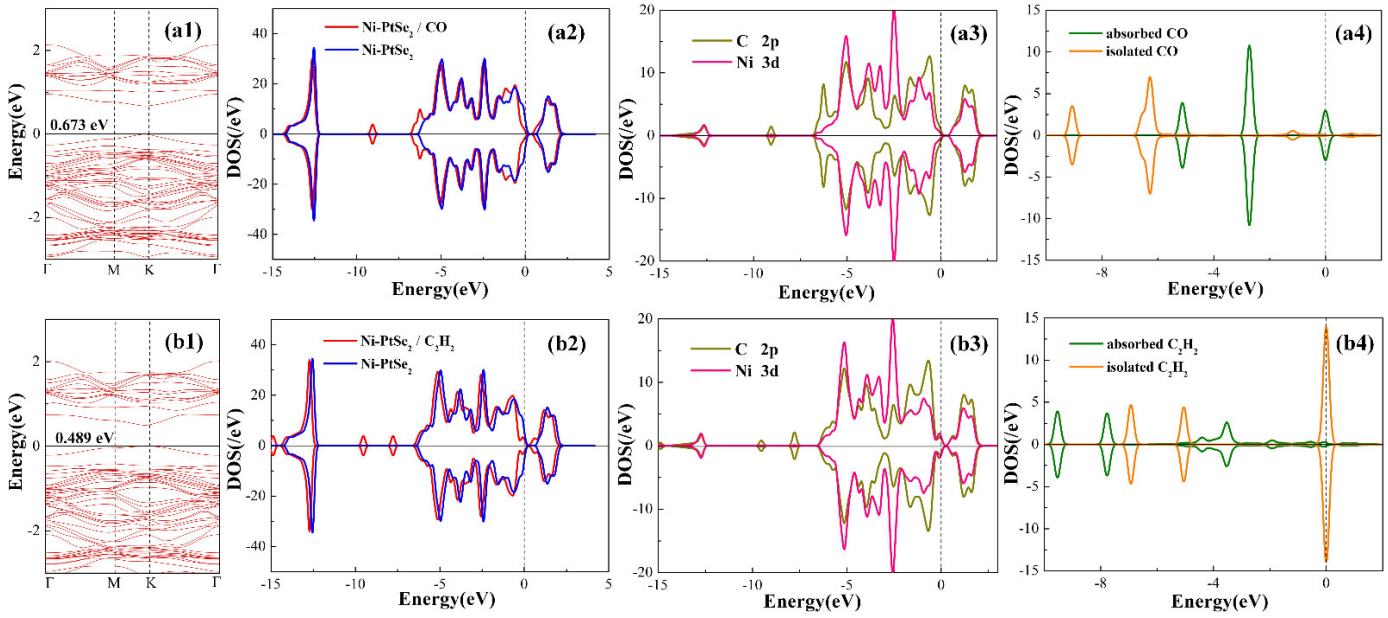

Figure 6. BS and DOS of (**a1**−**a4**) CO system and (**b1**−**b4**) C_2H_2 system. The dashed line is Fermi level.

The total DOS, orbital DOS, and molecular DOS of the gas before and after gas adsorption are displayed in Figure 6a2,a3,b2,b3. After the adsorption of various targeted molecules, one can see that the total DOS distributions of Ni-$PtSe_2$ monolayer, contain several deformations, where the curves are split into numerous novel small wave crests and left-shifted to a region, especially the CO adsorption system in Figure 6a2. The novel generated peaks are mainly located at −1.5, −6.25 and −9.0 eV in Figure 6a2 and 0.8, 0.5, −8.0 and −9.5 eV in Figure 6b2, respectively. Most of the BS curve in Figure 6b2, before and after C_2H_2 adsorption, almost overlaps, implying a stronger interaction for the CO system. These deformations may be put down to the orbital interaction between atoms bringing about the electrons on the gas molecules to activate and further alter the electronic behavior of the whole adsorption system. In other words, the novel generated peaks around the Fermi level turn out the strong chemical reactions between the gas molecules and Ni-$PtSe_2$ surface, which results in the formation of covalent bonds.

From the partial DOS in Figure 6a3,b3, where the orbital interactions occur between bonded atoms, namely the Ni dopant and the C atom of targeted molecules, the enormous overlaps are mainly located at −5.0, −1.2, and 1.2 eV in the CO system and at −5.1, −1.0, and 1.2 eV in the C_2H_2 system, indicating the strong orbital hybridization between Ni 3d orbital and C 2p orbital, and the strong binding force of Ni-C bonds. Otherwise, these overlaps of the two orbitals give rise to the deformations of the total DOS in large part, where several novel peaks emerge and occur at the offset of the curve position. Moreover, the scope of these overlaps between Ni 3d orbital and C 2p orbital in the CO adsorption system is larger than that in the C_2H_2 system, which verifies the stronger chemical interaction of the CO adsorption system.

On all accounts, stronger orbital interaction in the CO adsorption system can be confirmed by means of the above analysis, as consistent with the inference of gas adsorption configurations. The sensing mechanism of the Ni-$PtSe_2$ monolayer can be effectively explored in the dissolved gas of transformer oil on account of the change of electrical conductivity after gas adsorption.

3.4. Sensing Response and Recovery Property of Ni-$PtSe_2$ Monolayer

During the process of gas adsorption, the changes in the electronic behavior in various gas atmospheres correspond to respective conductivity responses, which are directly reflected in the value of the bandgap and provide the intuitive data to judge the sensing performance of the Ni-$PtSe_2$ monolayer. Furthermore, the variational electrical conductivity can result in the altered sensitivity of the Ni-$PtSe_2$ monolayer. We list the following two formulas for electrical conductivity (σ) and sensitivity (S) of the Ni-$PtSe_2$ surface to accurately capture the small change in the electronic behavior [10,22].

$$\sigma = A * e^{(-B_g/2kT)} \tag{2}$$

$$S = ({\sigma^{-1}}_{gas} - {\sigma^{-1}}_{pure})/{\sigma^{-1}}_{pure} = (\sigma_{pure} - \sigma_{gas})/\sigma_{gas} \tag{3}$$

where A is a constant, B_g is the bandgap, k is the Boltzmann constant and T is working temperature, while σ_{gas} and σ_{pure} mean the electrical conductivity of the gas absorption system and isolated Ni-$PtSe_2$ monolayer, respectively. Based on formula (2), the decreasing bandgap of the CO and C_2H_2 systems can give rise to the increase in electrical conductivity of the Ni-$PtSe_2$ monolayer, which provides the basic mechanism to explore the electrical conductivity of various adsorption systems for the Ni-$PtSe_2$ monolayer. However, the measure of separating the mixed gas needs to be carried out to realize efficient detection, since a sensing material cannot select certain gas in the mixed gas environment. According to the above formula calculation, the sensitivity of the Ni-$PtSe_2$ monolayer towards CO and C_2H_2 detection can reach up to 96.74% and 99.91% at room temperature (298 K), respectively, which not only exhibits the detailed conductivity values but also manifests the favorable sensing property of these gases as a chemical resistance-type sensor. Taken

together, it is a promising gas sensor for the Ni-$PtSe_2$ monolayer with high sensitivity to detect CO and C_2H_2 at room temperature.

Apart from that, the recovery time (τ) is also a critical parameter to judge the repeatability of the sensing material. The formula is shown below [10,22]:

$$\tau = A^{-1}e^{(-E_a/K_BT)} \quad (4)$$

where A is the attempt frequency (10^{12} s^{-1}), T is temperature, and K_B is the Boltzmann constant (8.314 × 10^{-3} kJ/(mol·K)) [28]. E_a is a potential barrier, which is equal to E_{ad} in this work. In other words, the recovery time of a sensing material is the time required for desorption. As exhibited in Figure 7, we list the various temperatures of 298, 448, and 598 K to contrast and analyze the desorption property of the Ni-$PtSe_2$ monolayer based on the impact of temperature on τ.

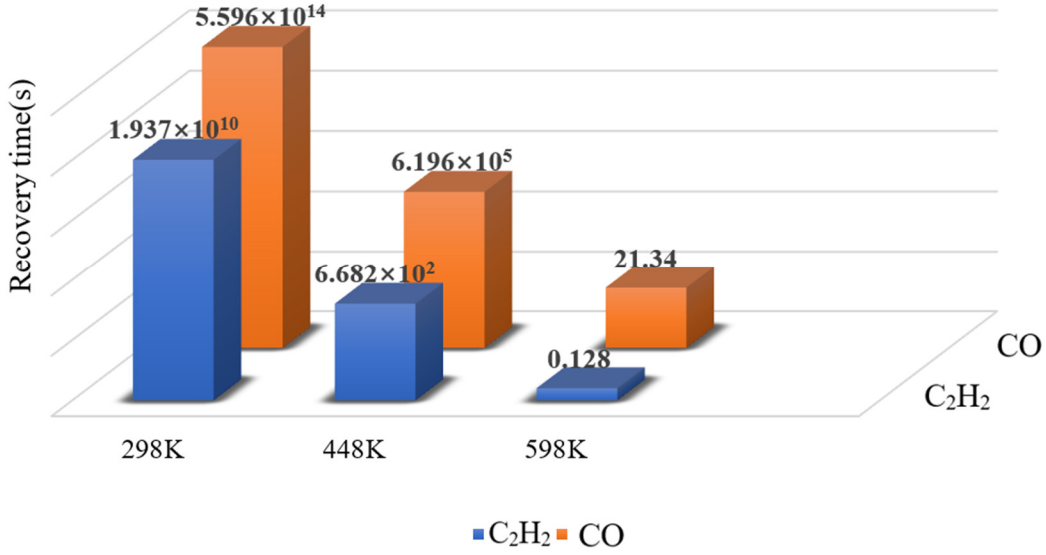

Figure 7. Recovery time for two species at various temperatures.

From Formula (4), it is obvious that T and E_a are the two significant parameters that affect the value of τ, where a lower E_a and a higher temperature will give rise to a smaller τ in the case of other parameters remaining the same, respectively. As portrayed in Figure 7, one can see that the desorption of CO and C_2H_2 from the Ni-$PtSe_2$ monolayer are rather tough at room temperature, while the recovery time drops along with the boosting of temperature. On the flip side, the long recovery time for CO and C_2H_2 desorption at room temperature also confirm their strong chemical adsorption strength. We can find that the recovery times in CO and C_2H_2 systems dive to 21.34 s and 0.128 s at 598 K, respectively, which implies that the Ni-$PtSe_2$ monolayer as a gas sensing material can be reusable with a temperature of 598 K for the detection of CO and C_2H_2. Beyond that, the recovery time with various temperatures in the C_2H_2 system is lower than that in the CO system as a result of the weaker binding force with the Ni-$PtSe_2$ monolayer. In the meantime, the longer desorption time for CO just illustrates the stronger chemisorption compared with C_2H_2. However, we must consider the thermostability of this material and the high energy consumption at high temperatures. The typical highest operating temperature of a transformer reaches around 60 to 90 degrees, namely 333 K to 363 K, approximately. Though the recovery time of CO and C_2H_2 adsorption systems between 60 and 90 degrees is not short, it can be improved by other means, such as increasing the operating temperature of the sensor, which will be further studied in depth later. Hence, the Ni-$PtSe_2$ monolayer is a satisfied gas scavenger upon the noxious gas dissolved in transformer oil, but its recovery time at room temperature is not satisfactory.

4. Conclusions

In this work, the theoretical analysis for the sensing performance of Ni-$PtSe_2$ monolayer towards two dissolved gases in transformer oil, namely CO and C_2H_2, is conducted by the first-principles theory in order to explore the potential of this novel material for enhancing the operation status of the transformer in power systems. We use a Ni atom as the dopant doped on the pure $PtSe_2$ surface to form the Ni-$PtSe_2$ supercell, and then simulate the adsorption of CO and C_2H_2 on the Ni-$PtSe_2$ monolayer to explore its adsorption performance. The main conclusions from the whole paper can be summed up as followed:

(1) The substituted Ni atom drops into the Se vacancy, which forms the optimized configuration.
(2) The sensing property of Ni-$PtSe_2$ monolayer toward the dissolved gas in transformer oil, namely CO and C_2H_2, is sorted in ascending order as CO > C_2H_2, where the E_{ad} of two gas systems are calculated as −1.583 eV and −1.319 eV, respectively, both classified as chemisorption, and the stronger interaction in the CO system is further verified by the BS and DOS analysis.
(3) This novel gas sensing material upon CO and C_2H_2 detection possesses high sensitivity, and the decreasing bandgap of the CO and C_2H_2 systems can bring on the increase in electrical conductivity of the Ni-$PtSe_2$ monolayer.
(4) Ni-$PtSe_2$ monolayer is a reusable gas scavenger for detecting CO and C_2H_2 removal from a transformer at 598 K, but its recoverability needs to be further explored and improved at room temperature.

In conclusion, the above findings in this theoretical work indicate that the Ni-$PtSe_2$ monolayer is a promising candidate for scavenging the noxious gas decomposed in transformer oil, which will be extremely meaningful for gas-sensing application in the electrical field and be of great reference significance for future researchers.

Author Contributions: Methodology, Z.W.; formal analysis, Z.W.; investigation, Z.W., G.Z., L.L., Y.W., J.W., S.X.; data curation, Z.W., L.L., J.W.; writing—original draft preparation, Z.W.; writing—review and editing, G.Z., L.L., Y.W., J.W., S.X.; supervision, G.Z., Y.W. All authors have read and agreed to the published version of the manuscript.

Funding: This work is supported by the Key Research and Development Program of Hubei Province, China (No. 2020BAA022) and Natural Science Foundation of Hubei Province (No. 2020CFB166).

Institutional Review Board Statement: Not applicable.

Informed Consent Statement: Not applicable.

Data Availability Statement: Not applicable.

Conflicts of Interest: The authors declare no conflict of interest.

References

1. Cui, H.; Zhang, X.; Zhang, J.; Zhang, Y. Nanomaterials-based gas sensors of SF_6 decomposed species for evaluating the operation status of high-voltage insulation devices. *High Volt.* **2019**, *4*, 242–258. [CrossRef]
2. Zhang, G.; Zhang, X.; Cheng, H.; Tang, J. Ladder-Wise calculation method for z-coordinate of transformer PD source based on planar layout UHF antenna sensors. *IEEJ Trans. Electr. Electron. Eng.* **2020**, *15*, 340–345. [CrossRef]
3. Cui, H.; Zhang, X.; Zhang, G.; Tang, J. Pd-doped MoS_2 monolayer: A promising candidate for DGA in transformer oil based on DFT method. *Appl. Surf. Sci.* **2019**, *470*, 1035–1042. [CrossRef]
4. Zhang, X.; Fang, R.; Chen, D.; Zhang, G. Using Pd-Doped gamma-Graphyne to Detect Dissolved Gases in Transformer Oil: A Density Functional Theory Investigation. *Nanomaterials* **2019**, *9*, 1490. [CrossRef] [PubMed]
5. Wu, Y.; Zhang, X.; Negi, A.; He, J.; Hu, G.; Tian, S.; Liu, J. Synergistic Effects of Boron Nitride (BN) Nanosheets and Silver (Ag) Nanoparticles on Thermal Conductivity and Electrical Properties of Epoxy Nanocomposites. *Polymers* **2020**, *12*, 426. [CrossRef] [PubMed]
6. Zhang, X.; Wu, Y.; Chen, X.; Wen, H.; Xiao, S. Theoretical Study on Decomposition Mechanism of Insulating Epoxy Resin Cured by Anhydride. *Polymers* **2017**, *9*, 341. [CrossRef] [PubMed]
7. Cui, H.; Zhang, G.; Zhang, X.; Tang, J. Rh-doped $MoSe_2$ as a toxic gas scavenger: A first-principles study. *Nanoscale Adv.* **2019**, *1*, 772–780. [CrossRef]

8. Wang, J.; Zhang, X.; Liu, L.; Wang, Z. Dissolved gas analysis in transformer oil using Ni-Doped GaN monolayer: A DFT study. *Superlattices Microstruct.* **2021**, *159*, 107055. [CrossRef]
9. Zhang, X.; Yu, L.; Wu, X.; Hu, W. Experimental sensing and density functional theory study of H_2S and SOF_2 adsorption on Au-modified graphene. *Adv. Sci.* **2015**, *2*, 1500101. [CrossRef] [PubMed]
10. Zhu, H.; Cui, H.; He, D.; Cui, Z.; Wang, X. Rh-doped $MoTe_2$ Monolayer as a Promising Candidate for Sensing and Scavenging SF6 Decomposed Species: A DFT Study. *Nanoscale Res. Lett.* **2020**, *15*, 129. [CrossRef]
11. Li, Z.; Chen, S.; Gong, S.; Feng, B.; Zhou, Z. Theoretical study on gas decomposition mechanism of SF_6 by quantum chemical calculation. *Comput. Theor. Chem.* **2016**, *1088*, 24–31. [CrossRef]
12. Wang, D.-W.; Wang, X.H.; Yang, A.J.; Chu, J.F.; Lv, P.L.; Liu, Y.; Rong, M.Z. $MoTe_2$: A Promising Candidate for SF_6 Decomposition Gas Sensors With High Sensitivity and Selectivity. *IEEE Electron Device Lett.* **2018**, *39*, 292–295. [CrossRef]
13. Lőrinczi, A.; Fagadar-Cosma, E.; Socol, G.; Mihăilescu, A.; Matei, E.; Sava, F.; Ştefan, M. $SnSe_2$-Zn-Porphyrin Nanocomposite Thin Films for Threshold Methane Concentration Detection at Room Temperature. *Chemosensors* **2020**, *8*, 134. [CrossRef]
14. Wang, Y.; Ding, D.; Zhang, Y.; Yuan, Z.; Tian, S.; Zhang, X. Research on Infrared Spectrum Characteristics and Detection Technology of Environmental-friendly Insulating Medium $C_5F_{10}O$. *Vib. Spectrosc.* **2022**, *118*, 103336. [CrossRef]
15. Wu, Y.; Ding, D.; Wang, Y.; Zhou, C.; Lu, H.; Zhang, X. Defect Recognition and Condition Assessment of Epoxy Insulators in Gas Insulated Switchgear Based on Multi-information Fusion. *Measurement* **2022**, *190*, 110701. [CrossRef]
16. Ma, D.; Wang, Q.; Li, T.; He, C.; Ma, B.; Tang, Y.; Lu, Z.; Yang, Z. Repairing sulfur vacancies in the MoS_2 monolayer by using CO, NO and NO2 molecules. *J. Mater. Chem. C* **2016**, *4*, 7093–7101. [CrossRef]
17. Chen, D.; Zhang, X.; Tang, J.; Cui, H.; Li, Y. Noble metal (Pt or Au)-doped monolayer MoS2 as a promising adsorbent and gas-sensing material to SO_2, SOF_2 and SO_2F_2: A DFT study. *Appl. Phys. A* **2018**, *124*, 194. [CrossRef]
18. Komsa, H.-P.; Kurasch, S.; Lehtinen, O.; Kaiser, U.; Krasheninnikov, A.V. From point to extended defects in two-dimensional MoS_2: Evolution of atomic structure under electron irradiation. *Phys. Rev. B* **2013**, *88*, 035301. [CrossRef]
19. Ma, D.; Ju, W.; Li, T.; Zhang, X.; He, C.; Ma, B.; Lu, Z.; Yang, Z. The adsorption of CO and NO on the MoS_2 monolayer doped with Au, Pt, Pd, or Ni: A first-principles study. *Appl. Surf. Sci.* **2016**, *383*, 98–105. [CrossRef]
20. Wei, H.; Gui, Y.; Kang, J.; Wang, W.; Tang, C. A DFT Study on the Adsorption of H(2)S and SO(2) on Ni Doped MoS(2) Monolayer. *Nanomaterials* **2018**, *8*, 646. [CrossRef]
21. Yoon, H.S.; Joe, H.E.; Jun Kim, S.; Lee, H.S.; Im, S.; Min, B.K.; Jun, S.C. Layer dependence and gas molecule absorption property in MoS_2 Schottky diode with asymmetric metal contacts. *Sci. Rep.* **2015**, *5*, 10440. [CrossRef] [PubMed]
22. Li, D.; Rao, X.; Zhang, L.; Zhang, Y.; Ma, S.; Chen, L.; Yu, Z. First-Principle Insight into the Ru-Doped $PtSe_2$ Monolayer for Detection of H_2 and C_2H_2 in Transformer Oil. *ACS Omega* **2020**, *5*, 31872–31879. [CrossRef] [PubMed]
23. Wang, Y.; Li, L.; Yao, W.; Song, S.; Sun, J.T.; Pan, J.; Ren, X.; Li, C.; Okunishi, E.; Wang, Y.-Q.; et al. Monolayer PtSe(2), a New Semiconducting Transition-Metal-Dichalcogenide, Epitaxially Grown by Direct Selenization of Pt. *Nano Lett.* **2015**, *15*, 4013–4018. [CrossRef] [PubMed]
24. Sajjad, M.; Montes, E.; Singh, N.; Schwingenschlögl, U. Superior Gas Sensing Properties of Monolayer $PtSe_2$. *Adv. Mater. Interfaces* **2017**, *4*, 1600911. [CrossRef]
25. Tian, S.; Zhang, X.; Cressault, Y.; Hu, J.; Wang, B.; Xiao, S.; Li, Y.; Kabbaj, N. Research status of replacement gases for SF_6 in power industry. *AIP Adv.* **2020**, *10*, 050702. [CrossRef]
26. Wang, J.; Zhang, X.; Liu, L.; Wang, Z. Adsorption of SF_6 Decomposition Products by the S Vacancy Structure and Edge Structure of SnS_2: A Density Functional Theory Study. *ACS Omega* **2021**, *6*, 28131–28139. [CrossRef]
27. Zhang, X.; Wang, J.; Chen, D.; Liu, L. The adsorption performance of harmful gas on Cu doped WS_2: A first-principle study. *Mater. Today Commun.* **2021**, *28*, 102488. [CrossRef]
28. Zhou, Q.; Zhang, G.; Tian, S.; Zhang, X. First-Principles Insight into Pd-Doped ZnO Monolayers as a Promising Scavenger for Dissolved Gas Analysis in Transformer Oil. *ACS Omega* **2020**, *5*, 17801–17807. [CrossRef]
29. Li, P.; Hong, Q.; Wu, T.; Cui, H. SOF_2 sensing by Rh-doped PtS_2 monolayer for early diagnosis of partial discharge in the SF_6 insulation device. *Mol. Phys.* **2021**, *119*, e1919774. [CrossRef]
30. Cui, H.; Zhang, X.; Li, Y.; Chen, D.; Zhang, Y. First-principles insight into Ni-doped InN monolayer as a noxious gases scavenger. *Appl. Surf. Sci.* **2019**, *494*, 859–866. [CrossRef]
31. Tkatchenko, A.; DiStasio, R.A., Jr.; Head-Gordon, M.; Scheffler, M. Dispersion-corrected Møller-Plesset second-order perturbation theory. *J. Chem. Phys.* **2009**, *131*, 171.
32. Fan, Y.; Zhang, J.; Qiu, Y.; Zhu, J.; Zhang, Y.; Hu, G.A. DFT study of transition metal (Fe, Co, Ni, Cu, Ag, Au, Rh, Pd, Pt and Ir)-embedded monolayer MoS_2 for gas adsorption. *Comput. Mater. Sci.* **2017**, *138*, 255–266. [CrossRef]
33. Cui, H.; Yan, C.; Jia, P.; Cao, W. Adsorption and sensing behaviors of SF6 decomposed species on Ni-doped C_3N monolayer: A first-principles study. *Appl. Surf. Sci.* **2020**, *512*, 145759. [CrossRef]
34. Aretouli, K.E.; Tsipas, P.; Tsoutsou, D.; Marquez-Velasco, J.; Xenogiannopoulou, E.; Giamini, S.A.; Vassalou, E.; Keladidis, N.; Dimoulas, A. Two-dimensional semiconductor $HfSe_2$ and $MoSe_2/HfSe_2$ van der Waals heterostructures by molecular beam epitaxy. *Appl. Phys. Lett.* **2015**, *106*, 699. [CrossRef]
35. Chen, D.; Zhang, X.; Tang, J.; Cui, Z.; Cui, H.; Pi, S. Theoretical Study of Monolayer PtSe2 as Outstanding Gas Sensor to Detect SF_6 Decompositions. *IEEE Electron Device Lett.* **2018**, *39*, 1405–1408. [CrossRef]

36. Zhang, J.; Yang, G.; Tian, J.; Ma, D.; Wang, Y. First-principles study on the gas sensing property of the Ge, As, and Br doped $PtSe_2$. *Mater. Res. Express* **2018**, *5*, 035037. [CrossRef]
37. Zhang, W.; Song, X.J.; Zhou, N.; Li, H.; Huang, J. Magnetism and magnetocrystalline anisotropy in vacancy doped and (non)metal adsorbed single-layer $PtSe_2$. *Comput. Mater. Sci.* **2017**, *129*, 171–177. [CrossRef]
38. Zhu, L.; Wang, J.; Liu, J.; Xu, Z.; Nasir, M.S.; Chen, X.; Wang, Z.; Sun, S.; Ma, Q.; Liu, J.; et al. In situ enrichment amplification strategy enabling highly sensitive formaldehyde gas sensor. *Sens. Actuators B Chem.* **2022**, *354*, 131206. [CrossRef]
39. Cui, H.; Zhang, X.; Chen, D.; Tang, J. Pt & Pd decorated CNT as a workable media for SOF_2 sensing: A DFT study. *Appl. Surf. Sci.* **2019**, *471*, 335–341.
40. Cui, H.; Zheng, K.; Xie, Z.; Yu, J.; Zhu, X.; Ren, H.; Wang, Z.; Zhang, F.; Li, X.; Tao, L.; et al. Tellurene Nanoflake-Based NO_2 Sensors with Superior Sensitivity and a Sub-Parts-per-Billion Detection Limit. *ACS Appl. Mater. Interfaces* **2020**, *12*, 47704–47713. [CrossRef]
41. Zhang, D.; Cao, Y.; Yang, Z.; Wu, J. Nanoheterostructure Construction and DFT Study of Ni-Doped In_2O_3 Nanocubes/WS_2 Hexagon Nanosheets for Formaldehyde Sensing at Room Temperature. *ACS Appl. Mater. Interfaces* **2020**, *12*, 11979–11989. [CrossRef] [PubMed]
42. Mishra, N.; Pandey, B.P.; Kumar, S. Impact of N_2O Gas Adsorption Upon Electronic Properties of 2D $MoSe_2$ Monolayer: A DFT Approach. *IEEE Sens. J.* **2021**, *21*, 9756–9762. [CrossRef]
43. Li, X.-H.; Cui, H.-L.; Zhang, R.-Z.; Li, S.-S. First-principles study of biaxial strain effect on NH_3 adsorbed Ti_2CO_2 monolayer. *Vacuum* **2020**, *179*, 109574. [CrossRef]